arXiv:1403.5008v1 [cond-mat.mtrl-sci] 20 Mar 2014

Magnetization Process of the $S = 1/2$ Heisenberg Antiferromagnet on the Cairo Pentagon Lattice

Hiroki Nakano[1] *, Makoto Isoda[2], † and Tôru Sakai[1,3] ‡,

[1] *Graduate School of Material Science, University of Hyogo, Kouto 3-2-1, Kamigori, Ako-gun, Hyogo 678-1297, Japan*
[2] *Department of Physics, Faculty of Education, Kagawa University Saiwai-cho 1-1, Takamatsu 760-8522, Japan*
[3] *Japan Atomic Energy Agency, SPring-8, Kouto 1-1-1, Sayo, Hyogo 679-5148, Japan*

(Received March 21, 2014)

We study the $S = 1/2$ Heisenberg antiferromagnet on the Cairo pentagon lattice by the numerical-diagonalization method. We tune the ratio of two antiferromagnetic interactions coming from two kinds of inequivalent sites in this lattice, examining the magnetization process of the antiferromagnet; particular attention is given to one-third of the height of the saturation. We find that quantum phase transition occurs at a specific ratio and that a magnetization plateau appears in the vicinity of the transition. The plateau is accompanied by a magnetization jump on one side among the edges due to the spin-flop phenomenon. Which side the jump appears depends on the ratio.

Frustration often plays an essential role in the behaviors of various magnetic materials, where exotic phenomena are induced owing to such frustration. Frustration occurs in magnets when the system includes a particular geometry of the structure. The systems of the kagome-lattice antiferromagnet, triangular-lattice antiferromagnet, and pyrochlore-lattice antiferromagnet which are typical frustrated magnets, are composed of local triangles creating a strong frustration. In spite of the fact that extensive studies have been carried out to understand these systems well, there remain unclear behaviors; investigations continue on from various viewpoints and by various methods until now.

However, there are only a few studies of systems that are composed of nontriangular local structures. Since frustration occurs when bonds of antiferromagnetic interaction form an odd-number polygon, the next candidate is a pentagon. Under such circumstances, $Bi_2Fe_4O_9$ in Ref. 1 and $Bi_4Fe_5O_{13}F$ in Ref. 2 were studied; there are materials of an antiferromagnet on a lattice composed of pentagons. The lattice is called the Cairo pentagon lattice, which is shown in Fig. 1. Although an Fe^{3+} ion in these materials behaves as an $S = 5/2$ spin, from the theoretical point of view, a numerical-diagonalization investigation of the $S = 1/2$ antiferromagnet on this lattice was carried out.[3] The behavior under an external magnetic field, however, is not understood sufficiently.

In the present letter, we report our study of the magnetization process of the $S = 1/2$ Heisenberg antiferromagnet on a Cairo pentagon lattice by the numerical-diagonalization method while the ratio of two antiferromagnetic interactions in the system is varied. Particularly, we focus our attention on the behavior around the one-third height of the saturation. Extensive studies of this model in the entire range of the ratio will be published elsewhere.[4] The purpose of the present study is to clarify the changes in the behavior with the variation in the ratio. We report a marked change around a particular ratio, which is accompanied by a spin-flop phenomenon in a system without spin anisotropy.

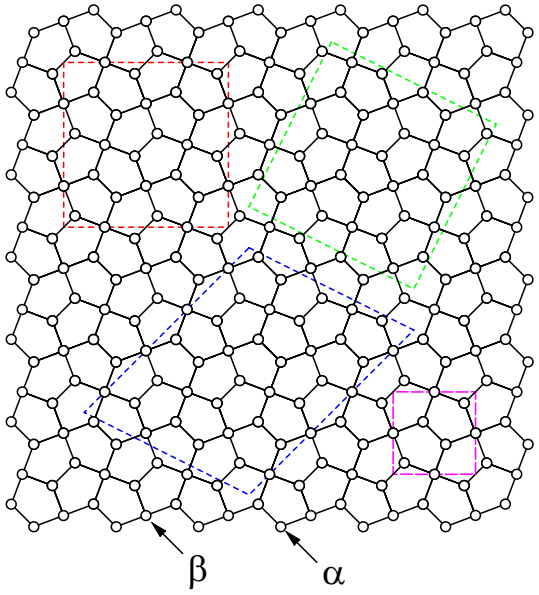

Fig. 1. (Color) Cairo pentagon lattice and its finite-size clusters. The small violet square composed of long-dashed lines illustrates a unit cell of the Cairo pentagon lattice. α and β denote a site with the coordination numbers $z = 3$ and $z = 4$, respectively. Red square, green tilted square, and blue parallelogram composed of dotted lines denote a finite-size cluster for $N_s = 24$, 30, and 36, respectively.

Before we present our new results, let us review the features of the Cairo pentagon lattice. Vertices of pentagons in the Cairo pentagon lattice are divided into two groups: one is a vertex with a coordination number $z = 3$ and the other is a vertex with $z = 4$, which are hereafter called the α and β sites, respectively. Note here that there are two types of bonds connecting the two neighboring vertices: α-α and α-β bonds. The unit cell of the lattice shown in Fig. 1 include six sites, among which there are

*E-mail address: hnakano@sci.u-hyogo.ac.jp
†E-mail address: misoda@ed.kagawa-u.ac.jp
‡E-mail address: sakai@spring8.or.jp

four α and two β sites.

The Hamiltonian studied in this research is given by $\mathcal{H} = \mathcal{H}_0 + \mathcal{H}_{\rm Zeeman}$, where

$$\mathcal{H}_0 = \sum_{\langle i,j\rangle\in\alpha\text{-}\alpha \text{ bonds}} J\boldsymbol{S}_i\cdot\boldsymbol{S}_j + \sum_{\langle i,j\rangle\in\alpha\text{-}\beta \text{ bonds}} J'\boldsymbol{S}_i\cdot\boldsymbol{S}_j. \tag{1}$$

Let us emphasize here that $\mathcal{H}_0$ is isotropic in spin space. $\mathcal{H}_{\rm Zeeman}$ is given by

$$\mathcal{H}_{\rm Zeeman} = -h\sum_j S_j^z. \tag{2}$$

Here, $\boldsymbol{S}_i$ denotes the $S = 1/2$ spin operator at site i shown by circles in Fig. 1. Energies are measured in units of J for the lattice shown in Fig. 1(b); hereafter, we set $J = 1$. The number of spin sites is denoted by $N_{\rm s}$. We investigate how the magnetization process of the above model changes when the ratio $\eta = J'/J$ is tuned.

We calculate the lowest energy of $\mathcal{H}_0$ in the subspace belonging to $\sum_j S_j^z = M$, using numerical diagonalizations based on the Lanczos algorithm and/or the householder algorithm. Here, M takes an integer from zero to the saturation value $M_{\rm s}$ $(= SN_{\rm s})$. The energy is denoted by $E(N_{\rm s}, M)$. Lanczos diagonalizations have been carried out using the MPI-parallelized code, which was originally developed in the study of the Haldane gaps.[5] The usefulness of our program was confirmed in large-scale parallelized calculations.[6,7]

For a finite-size system, the magnetization process is determined by the magnetization increase from M to $M+1$ at the field

$$h = E(N_{\rm s}, M+1) - E(N_{\rm s}, M), \tag{3}$$

under the condition that the lowest-energy state with the magnetization M and that with $M+1$ become the ground state in specific magnetic fields. When the lowest-energy state with the magnetization M does not become the ground state in any field, the magnetization process around the magnetization M is determined by the Maxwell construction. In this study, we treat the finite-size clusters of $N_{\rm s} = 24$, 30, and 36 shown in Fig. 1. The periodic boundary condition is imposed for each cluster.

Let us, first, examine the magnetization process of the present model. When we tune η, we discover that a significant change in the behavior of the magnetization process appears at approximately $\eta = 0.8$. To observe the change, we depict our results for $\eta = 0.71$ and 0.85 in Fig. 2. In the one-third height of the saturation on which we focus our attention, one observes the presence of the magnetic plateau as a characteristic behavior. As a surprising feature, there also exists a magnetization jump at the *higher*-field edge of the plateau for $\eta = 0.71$, while a similar jump appears at the *lower*-field edge of the plateau for $\eta = 0.85$. Note here that a marked change in the magnetization process is induced only owing to a small change in η. The presence of the jump was pointed out in Ref. 3; the authors of Ref. 3 speculated that the behavior originated from the spin-nematic state because of $\Delta M = 2$ at the jump. In the present study, on the other hand, we investigate this behavior of the present model from the viewpoint of the spin-flop phenomenon[8–10] to understand the origin of the marked change.

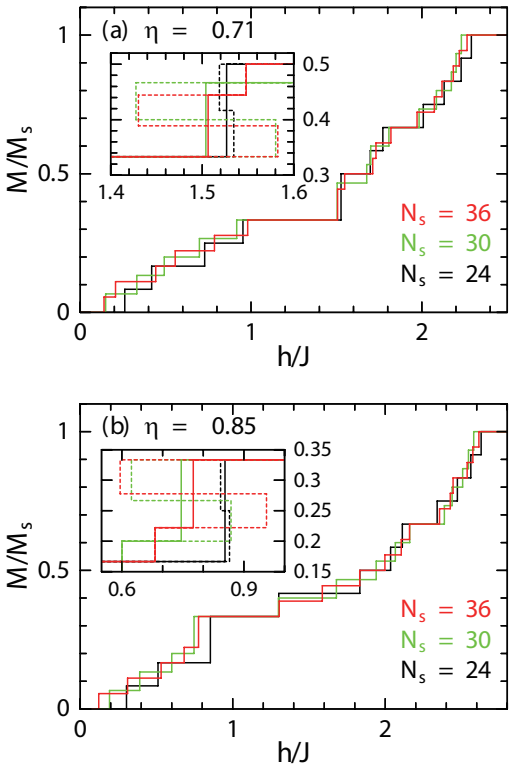

Fig. 2. (Color) Magnetization process of the $S = 1/2$ Heisenberg antiferromagnet on the Cairo pentagon lattice. The results for $\eta = 0.71$ and 0.85 are presented in (a) and (b), respectively. Black, green, and red lines denote the results for $N_{\rm s} = 24$, 30, and 36, respectively. Insets show a zoomed-in view at the higher (lower)-field edge of the one-third height of the saturation when $\eta = 0.71(0.85)$, where the dotted lines represent the results before the Maxwell construction is carried out.

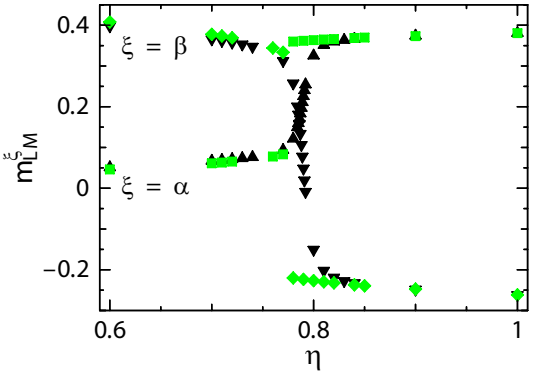

Fig. 3. (Color) Dependence of the average local magnetization on the ratio of interaction η. For $N_{\rm s} = 24$, triangles and inversed triangles denote the results of $\xi = \alpha$ and β, respectively. For $N_{\rm s} = 30$, squares and diamonds denote the results and $\xi = \alpha$ and β, respectively.

For this purpose, we examine the average local magnetization at the one-third height of the saturation. The average local magnetization is evaluated by

$$m_{\rm LM}^{\xi} = \frac{1}{N_\xi}\sum_{j\in\xi}\langle S_j^z\rangle, \tag{4}$$

where ξ takes α and β. Here, the symbol $\langle\mathcal{O}\rangle$ denotes the expectation value of an operator $\mathcal{O}$ with respect to the lowest-energy state within the subspace with a fixed M of interest. Note that the average over ξ is carried out in the case of degenerate ground states for some values of M, where N_ξ denotes the number of ξ sites. For M with a nondegenerate ground state, the results do not change irrespective of the presence or absence of the average. Our results of the η dependence of $m^\xi_{\rm LM}$ at $M/M_{\rm s}=1/3$ are shown in Fig. 3. One clearly observes a large decrease in $m^\beta_{\rm LM}$ and a large increase in $m^\alpha_{\rm LM}$ near $\eta=0.78$. However, we will publish the phase diagram under a nonzero magnetic field in a wide range of η in Ref. 4; here, we focus our attention only on the behavior near $\eta=0.78$ and we mention the phases around there with some relationships. In the region of η larger than this value, one observes in Fig. 3 that an α-site spin becomes an up-spin while a β-site spin becomes a down-spin. Note that a ground state under $h=0$ is exactly ferrimagnetic in the limiting case of $\eta\to\infty$. It is also known that the spontaneous magnetized phase of ferrimagnetism is spread for $\eta\gtrsim 1.96$, which was reported in Ref. 3. The present spin arrangement suggests that the state is in the ferrimagnetic phase *under a nonzero magnetic field*. In the region of smaller η, on the other hand, an α-site spin becomes almost vanishing, while a β-site spin becomes an up-spin. One finds that the vanishing moments at α sites suggest that orthogonal singlet dimers are formed at a pair of neighboring α spins[11] if it is considered that, in the case of $\eta=0$, the model is reduced to a system composed of isolated single spins at β sites and isolated dimers of antiferromagnetically interacting spins at α sites. The present results of a marked change of spin states strongly suggest that a quantum phase transition occurs at a specific η and that the characteristics of the magnetization plateau at $M/M_{\rm s}=1/3$ are different between the cases of $\eta=0.71$ and 0.85 observed in Fig. 2. Unfortunately, it is difficult to know the boundary point more precisely by extrapolating the results for finite-size clusters in the present study. Furthermore, it is also difficult to conclude whether the transition is of the second order or first order because the change in $m^\xi_{\rm LM}$ is continuous for $N_{\rm s}=24$, while it is discontinuous for $N_{\rm s}=30$. Even though such issues remain unresolved at the present stage, a quantum phase transition certainly occurs near $\eta=0.78$.

Next, let us study what happens in the appearance of the above magnetization jump as a result of the presence of the phase transition. For this purpose, we observe the $M/M_{\rm s}$ dependence of $m^\xi_{\rm LM}$ in the cases of $\eta=0.71$ and 0.85; the results are shown in Fig. 4. In the case of $\eta=0.71$, the dependences of $m^\xi_{\rm LM}$ for $M/M_{\rm s}<1/3$ seem continuous to those of $m^\xi_{\rm LM}$ at $M/M_{\rm s}=1/3$ while the dependences of $m^\xi_{\rm LM}$ for $M/M_{\rm s}>1/3$ seem discontinuous to those of $m^\xi_{\rm LM}$ at $M/M_{\rm s}=1/3$, even though we do not take the open-symbol data for energetically unrealized states into account. This discontinuity indicates an abrupt change in the spin orientation between the cases of $M/M_{\rm s}=1/3$ and $M/M_{\rm s}>1/3$, which is the origin of the magnetization jump as a consequence of the spin-flop phenomenon. Note that such phenomena occur in

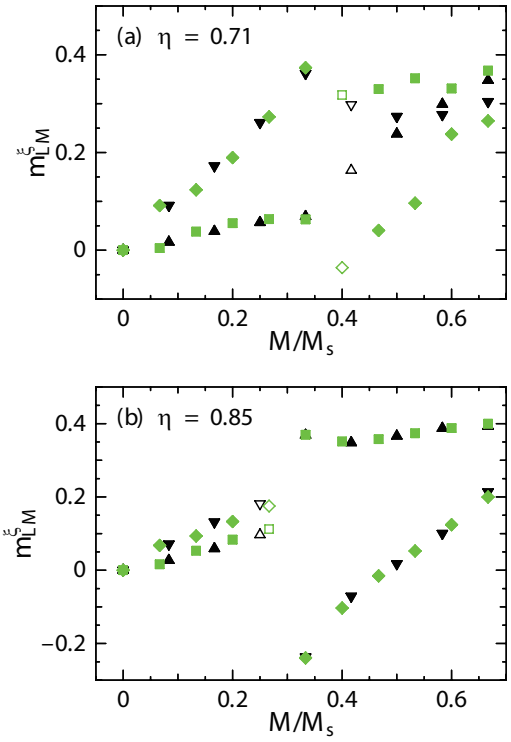

Fig. 4. (Color) Dependence of the average local magnetization on the total magnetization. The result of $\eta=0.71$ and 0.85 are shown in (a) and (b), respectively. The shapes of the symbols are the same as those in Fig. 3. Closed symbols represent data for the stably realized states, while open symbols denote data for the unstable states at the magnetization jump.

spite of the fact that the present system does not include any anisotropy in spin space. Such spin-flop phenomena in systems with the same spin-isotropic nature have recently been reported[12] in antiferromagnets on a square-kagome lattice[13–15] and a $\sqrt{3}\times\sqrt{3}$-distorted kagome lattice.[16,17] In the case of $\eta=0.85$, on the other hand, the dependences of $m^\xi_{\rm LM}$ for $M/M_{\rm s}>1/3$ seem continuous to those of $m^\xi_{\rm LM}$ at $M/M_{\rm s}=1/3$, while the dependences of $m^\xi_{\rm LM}$ for $M/M_{\rm s}<1/3$ seem discontinuous to those of $m^\xi_{\rm LM}$ at $M/M_{\rm s}=1/3$. One finds a change on one side of the edges where the discontinuous behavior appears in the spin orientation. The change also affects the appearance of the magnetization jump, as shown in Fig. 2. The key to understanding the dependence of the behavior on η is the difference between $m^\xi_{\rm LM}$ of $M/M_{\rm s}>1/3$ and that of $M/M_{\rm s}<1/3$. Although $m^\xi_{\rm LM}$ on both sides of the vicinity of $M/M_{\rm s}=1/3$ tries to catch up with the quite rapidly changing $m^\xi_{\rm LM}$ just at $M/M_{\rm s}=1/3$, the catching up cannot necessarily be realized on both sides of $M/M_{\rm s}>1/3$ and $M/M_{\rm s}<1/3$. The present result in the case of $\eta=0.85$ also suggests that the spin-flop phenomenon in a spin-isotropic system can occur not only at the higher-field edge of the one-third height of the saturation. It should be investigated in future studies whether or not the same phenomenon occurs at other heights of the saturation.

Similar magnetization jumps of $\Delta M=2$ are known in two finite-size systems without anisotropies in spin

space: one is the Heisenberg cluster on an icosaheron[18] and the other is the Heisenberg cluster on a dodecahedron.[19] Within the condition that one considers regular polyhedra, unfortunately, it is impossible to increase the number of spins systematically to that of an infinite system. The jumps in the two finite-size clusters necessarily appear between finite-size plateaux, although the widths of the plateaux beside the jump in the dodecahedron system are significantly larger than the widths of other finite-size plateaux in the same system. With this point of view, the situation is contrast to the behavior of the present model where no indication of the magnetization plateau in the thermodynamic limit of $N \to \infty$ is observed on the *opposite* side of a clearly existing magnetization plateau with respect to the jump. The jump of the icosaheron system appears only for a large spin amplitude of $S = 4$, while no jump is observed in the case of $S < 4$. Future studies of the Cairo-pentagon-lattice antiferrmagnet composed of larger spins would make it possible to examine the relationship between the icosaheron system and the present model.

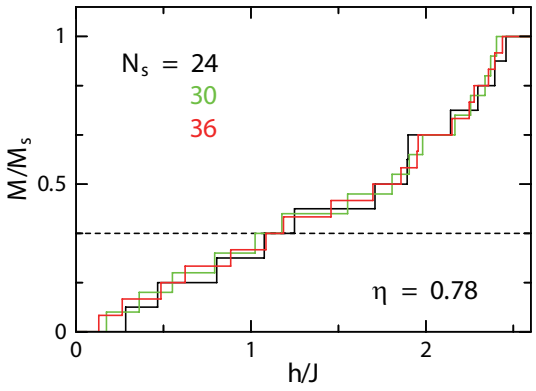

Fig. 5. (Color) Magnetization process of the Cairo-pentagon-lattice antiferromagnet with a ratio of $\eta = 0.78$. Black, green, and red lines denote the results for $N_s = 24$, 30, and 36, respectively.

Finally, let us observe the magnetization process around the boundary of the phase transition of $M/M_s = 1/3$. We depict the result of the magnetization process at $\eta = 0.78$ in Fig. 5. No jumps are observed. One finds that the width of the finite-size step at $M = (1/3)M_s$ is very small in comparison with the widths of those for $\eta = 0.71$ and 0.85 in Fig. 2. Within the result of $\eta = 0.78$, the width is also smaller than the widths of steps at $M = (1/3)M_s + 1$ and $M = (1/3)M_s - 1$. The small width suggests the disappearance of the magnetic plateau. However, a careful extrapolation toward the thermodynamic limit should be performed; this is an open issue in future studies.

In summary, we have investigated the magnetization process of the $S = 1/2$ Heisenberg antiferromagnet on the Cairo pentagon lattice by the numerical-diagonalization method with a variation in the ratio of the two antiferromagnetic interactions. We have found that a quantum phase transition occurs at the one-third height of the saturation. We have also found that a magnetization jump appears due to the spin-flop phenomenon. The present model is the first case when the spin-flop phenomenon without spin anisotropy occurs in a system that does not include a local lattice structure of triangles. Our unexpected observation is that the side where the jump appears depends on which side of the transition the ratio is located. The behavior of the Cairo-pentagon-lattice antiferromagnet is quite a characteristic behavior. Examinations of the comparison between other frustrated systems including antiferromagnets on the kagome lattice,[17,20] triangular lattice,[21] and interpolated case,[22,23] as well as on the square-kagome lattice[12] would provide us with various viewpoints that will contribute much to our understanding of frustration effects.

Acknowledgments

We wish to thank Professor Y. Hasegawa, Dr. T. Momoi, and Dr. N. Todoroki for fruitful discussions. This work was partly supported by Grants-in-Aid (Nos. 23340109, 23540388, and 24540348) from the Ministry of Education, Culture, Sports, Science and Technology of Japan (MEXT). Some of the computations were performed using facilities of the Department of Simulation Science, National Institute for Fusion Science; Center for Computational Materials Science, Institute for Materials Research, Tohoku University; the Supercomputer Center, Institute for Solid State Physics, The University of Tokyo; and Supercomputing Division, Information Technology Center, The University of Tokyo. This work was partly supported by the Strategic Programs for Innovative Research, MEXT, and the Computational Materials Science Initiative, Japan. The authors would like to express their sincere thanks to the staff members of the Center for Computational Materials Science of the Institute for Materials Research, Tohoku University for their continuous support of the SR16000 supercomputing facilities.

1) E. Ressouche, V. Simonet, B. Canals, M. Gospodinov, and V. Skumryev, Phys. Rev. Lett. **103**, 267204 (2009).
2) A. M. Abakumov, D. Batuk, A. A. Tsirlin, C. Prescher, L. Dubrovinsky, D. V. Sheptyakov, W. Schnelle, J. Hadermann, and G. V. Tendeloo1, Phys. Rev. Lett. **87**, 024423 (2013).
3) I. Rousochatzakis, A. M. Läuchli, and R. Moessner, Phys. Rev. B **85**, 104415 (2012).
4) M. Isoda, H. Nakano, and T. Sakai, submitted to J. Phys. Soc. Jpn.
5) H. Nakano and A. Terai, J. Phys. Soc. Jpn. **78**, 014003 (2009).
6) H. Nakano and T. Sakai, J. Phys. Soc. Jpn. **80**, 053704 (2011).
7) H. Nakano and T. Sakai, J. Phys. Soc. Jpn. **82**, 043715 (2013).
8) L. Néel, Ann. Phys. Paris **5**, 232 (1936).
9) M. Kohno and M. Takahashi, Phys. Rev. B **56**, 3212 (1997).
10) T. Sakai and M. Takahashi, Phys. Rev. B **60**, 7295 (1999).
11) This state is also similar to the inverse-T state in the square-kagome-lattice antiferromagnet in Ref. 12.
12) H. Nakano and T. Sakai, J. Phys. Soc. Jpn. **82**, 083709 (2013).
13) R. Siddharthan and A. Georges: Phys. Rev. B **65** (2001) 014417.
14) P. Tomczak and J. Richter, J. Phys. A: Math. Gen. **36**, 5399 (2003).
15) J. Richter, J. Schulenburg, P. Tomczak, and D. Schmalfuß, Condens. Matter Phys. **12**, 507 (2009).

16) H. Nakano, T. Sakai, and Y. Hasegawa, submitted to J. Phys. Soc. Jpn.
17) K. Hida, J. Phys. Soc. Jpn. **70**, 3673 (2001).
18) C. Schröder, H. J. Schmidt, J. Schnack, and M. Luban, Phys. Rev. Lett. **94**, 207203 (2005).
19) N. P. Konstantinidis, Phys. Rev. B **72**, 064453 (2005).
20) H. Nakano and T. Sakai, J. Phys. Soc. Jpn. **79**, 053707 (2010).
21) T. Sakai and H. Nakano, Phys. Rev. B **83**, 100405(R) (2011).
22) H. Nakano and T. Sakai, Phys. Status Solidi B **250**, 579 (2013).
23) H. Nakano and T. Sakai, to be published in JPS Conf. Proc.